

## Assessing the regional disparities in geoengineering impacts

Peter J. Irvine,<sup>1</sup> Andy Ridgwell,<sup>1</sup> and Daniel J. Lunt<sup>1,2</sup>

Received 23 June 2010; revised 16 August 2010; accepted 23 August 2010; published 28 September 2010.

[1] Solar Radiation Management (SRM) Geoengineering may ameliorate many consequences of global warming but also has the potential to drive regional climates outside the envelope of greenhouse-gas induced warming, creating ‘novel’ conditions, and could affect precipitation in some regions disproportionately. Here, using a fully coupled climate model we explore some new methodologies for assessing regional disparities in geoengineering impacts. Taking a  $4 \times \text{CO}_2$  climate and an idealized ‘sunshade’ SRM strategy, we consider different fractions of the maximum theoretical,  $4 \times \text{CO}_2$ -cancelling global mean cooling. Whilst regional predictions in particularly relatively low resolution global climate models must be treated with caution, our simulations indicate that it might be possible to identify a level of SRM geoengineering capable of meeting multiple targets, such as maintaining a stable mass balance of the Greenland ice sheet and cooling global climate, but without reducing global precipitation below pre-industrial or exposing significant fractions of the Earth to ‘novel’ climate conditions.

**Citation:** Irvine, P. J., A. Ridgwell, and D. J. Lunt (2010), Assessing the regional disparities in geoengineering impacts, *Geophys. Res. Lett.*, 37, L18702, doi:10.1029/2010GL044447.

### 1. Introduction

[2] Geoengineering has been proposed as a means to reduce surface greenhouse-induced warming and help avert discontinuous state transitions in the Earth system (known loosely as ‘tipping points’ [Lenton *et al.*, 2008]) and dangerous climate change [Hansen *et al.*, 2006]. Solar Radiation Management (SRM) geoengineering, through intervention with various components of the incoming solar radiation budget, restricts the amount of shortwave radiation absorbed by the Earth’s surface [Lenton and Vaughan, 2009]. An advantage of SRM is that it could produce a relatively rapid cooling compared to traditional mitigation or carbon capturing geoengineering [Lenton and Vaughan, 2009; Robock *et al.*, 2009]. Hence, while it does not address geochemical impacts of elevated atmospheric  $\text{CO}_2$  such as ocean acidification [Matthews *et al.*, 2009; Robock *et al.*, 2009], SRM has thus attracted attention particularly in the context of an ‘emergency’ mitigation option.

[3] General Circulation Model (GCM) studies of large scale SRM geoengineering schemes, such as the creation of a solar ‘sunshade’ [Angel, 2006] or stratospheric sulphate aerosol injection [Crutzen, 2006] have revealed that a globally uniform intervention cannot cancel out the pattern

of warming that elevated  $\text{CO}_2$  creates [Brovkin *et al.*, 2009; Govindasamy *et al.*, 2003; Lunt *et al.*, 2008]. Even for a perfect correction for the global mean surface air temperature, the poles are left relatively warmer and the Equator cooler due to differences in the zonal distributions of short and long wave radiation budget [Govindasamy *et al.*, 2003; Lunt *et al.*, 2008]. Adverse impacts of SRM geoengineering on the hydrological cycle may be more serious, with most simulations indicating a global reduction in precipitation with more acute changes regionally [Bala *et al.*, 2008; Lunt *et al.*, 2008]. The potential to exacerbate droughts (or floods) beyond the effects of elevated  $\text{CO}_2$  alone makes the consideration of SRM geoengineering technologies controversial [Bala *et al.*, 2008; Robock *et al.*, 2009].

[4] The nature and patterns of the climatic (and ultimately, socio-economic) impact of geoengineering must hence be understood for adequately informed decision making on potential SRM implementation. In this paper we explore different ways in which regional disparities in geoengineering impacts can be assessed in a fully coupled climate model. However, it must be borne in mind that GCMs, whilst being the best available tools (short of large-scale field trials and partial deployment) to assess the likely impacts of SRM geoengineering, currently do not perform well on the regional scale and particularly not for precipitation [Intergovernmental Panel on Climate Change (IPCC), 2007].

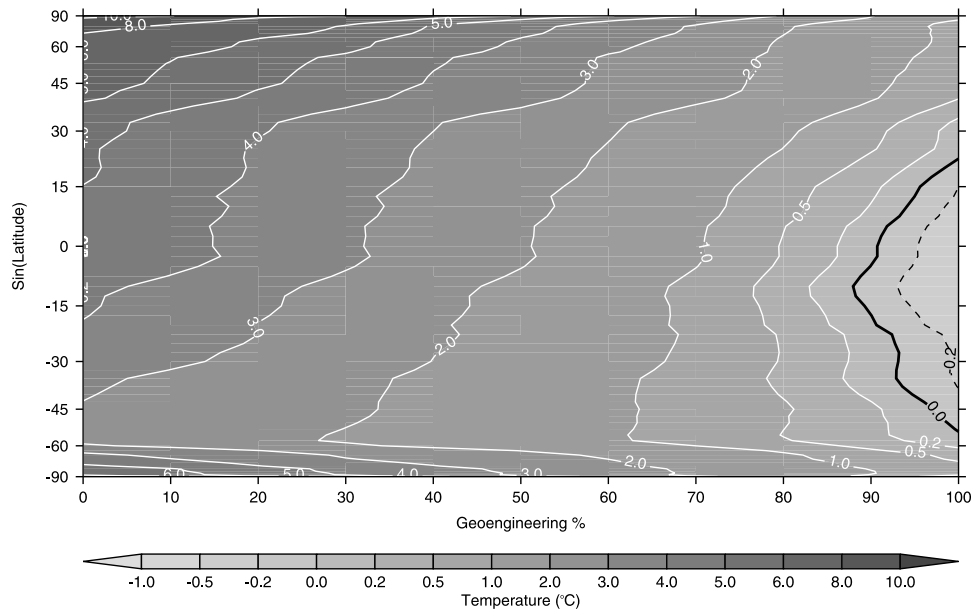
### 2. Methodology

[5] We used the fully coupled atmosphere-ocean UK Met Office GCM, HadCM3L [Cox *et al.*, 2000] in a configuration identical to that described by Lunt *et al.* [2008]. With this, we carried out twelve 400-year climate model simulations, all initialized from the end of a (pre-industrial) spin-up totaling more than 1000 years, with the final 100 years used to calculate the climatological averages. Of these, three followed Lunt *et al.* [2008] – a pre-industrial control (‘Pre’), a simulation with atmospheric  $\text{CO}_2$  set at 1120 ppmv, i.e., 4 times the pre-industrial value (‘0%Geo’), and a simulation with 1120 ppmv but reduced solar constant (‘100%Geo’). In 100%Geo (full SRM), the reduction in the solar constant is chosen such that the global annual mean 2m air temperature is as close as possible to that of the Pre simulation and determined iteratively [Lunt *et al.*, 2008]. For 100%Geo, the solar constant is  $57 \text{ Wm}^{-2}$  less than that of Pre, a reduction of 4.2%. A further nine simulations were carried out; all at 1120ppmv  $\text{CO}_2$  but differing in that the solar constant is reduced by a fraction of the maximum 100%Geo value from 10% to 90% in increments of 10%. It should be recognized that these simulations are not intended to represent realistic scenarios of future climate or geoengineering mitigation *per se*, but instead are designed to illustrate the effect of degrees

<sup>1</sup>Bristol Research Initiative for the Dynamic Global Environment, School of Geographical Sciences, University of Bristol, Bristol, UK.

<sup>2</sup>British Antarctic Survey, Cambridge, UK.

## A - Zonal SAT Anomaly



## B - Zonal Precipitation Anomaly

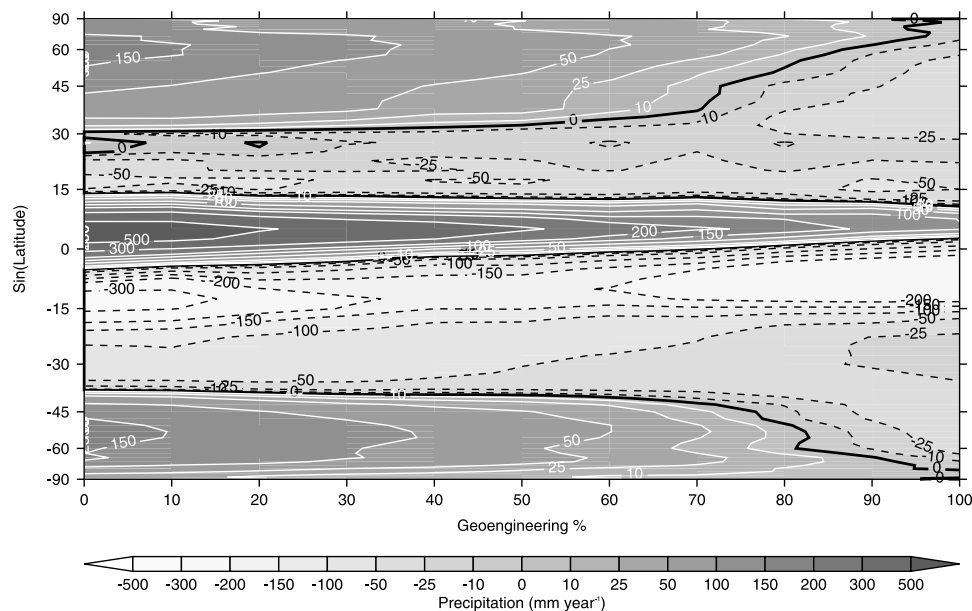


**Figure 1.** Zonally averaged anomaly with pre-industrial control. (a) Mean annual surface air temperature (SAT) and (b) precipitation. Plots show the sine of latitude (to facilitate comparison on a per-area impacted basis) against the level of SRM geoengineering.

of SRM geoengineering on a high- $\text{CO}_2$  world and how the spatial patterns of impact might change.

### 3. Results

[6] As previously noted [e.g., *Govindasamy et al.*, 2003; *Brovkin et al.*, 2009; *Lunt et al.*, 2008], we find that SRM does not perfectly cancel the warming due to elevated  $\text{CO}_2$  levels, even when prescribing a reduction in the solar constant sufficient to return the global average surface temperature to pre-industrial (Figure 1a). With an increasing

degree of SRM geoengineering deployment, surface air temperatures (SAT) decrease, with higher latitudes cooling more than lower latitudes. For full SRM deployment (100% *Geo*), annual SAT at the Equatorial regions becomes cooler than pre-industrial ( $\sim -0.5^\circ\text{C}$ ) while the poles remain warmer ( $\sim +1^\circ\text{C}$ ). This temperature difference between the Polar Regions and the Equatorial regions arises due to the spatial difference between the radiative forcing effect of the reduced insolation and the raised  $\text{CO}_2$  levels and is amplified by the operation of temperature feedbacks involving snow cover and sea-ice extent.

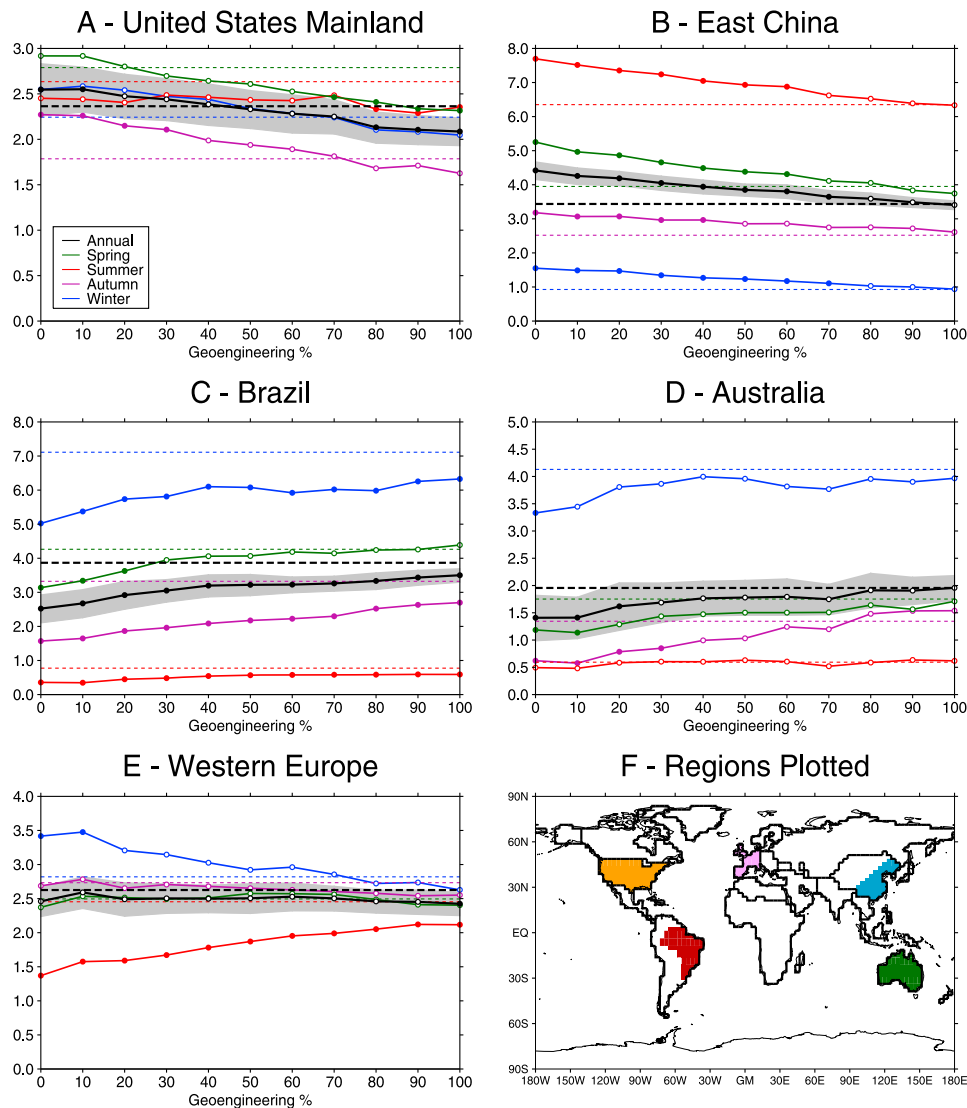


**Figure 2.** (a–e) The average daily rainfall in mm per day, both seasonally and annually, as a function of the level of geoengineering. The shaded region shows  $\pm$  one standard deviation around the annual mean at each level of geoengineering. The pre-industrial average is shown with a thick dashed line for the annual average and with thin dashed lines for each season. Unfilled circles show which values are within  $\pm$  one standard deviation of the pre-industrial level and filled circles show values that are outside of this range (i.e., more than 1 s.d. from pre-industrial). (f) The regions plotted and the borders of the FUND regions on which they are based [Anthoff *et al.*, 2009].

[7] The response of the zonal average precipitation anomaly as a function of the level of SRM is more complex (Figure 1b). In the simulated unmitigated  $4 \times \text{CO}_2$  climate ( $0\% \text{Geo}$ ), we find substantial changes in hydrology which are broadly consistent with other fully coupled climate models [IPCC, 2007] – increases in precipitation in the tropics and high latitudes and decreases in the sub-tropics. For the three wetter bands (Tropical, extra-tropical, and Polar), increasing the level of SRM decreases precipitation, and in the  $100\% \text{Geo}$  experiment, the extra-tropical regions end up drier and the tropics wetter than in the pre-industrial. In the southern subtropical zone between  $10\text{S}$  and  $15\text{S}$ , we observe a maximum in precipitation at  $\sim 50\%$  deployment and reduced precipitation at  $0\% \text{Geo}$  and  $100\% \text{Geo}$ .

[8] However, aggregating geoengineering climatic changes into zonal and annual averages hides a more complex and heterogeneous pattern of geoengineering impacts. To

visualize this we have defined a series of averaging regions, consisting of grouped national boundaries (but which are further subdivided to avoid averaging over disparate climate conditions) and based on those from the FUND model (Figure 2f). For illustration, here we show the change in annual and seasonal (Northern Hemisphere seasons, e.g. June, July and August for summer, etc.) precipitation for five different regions (Figure 2).

[9] We find that the United States mainland region shows the closest match to global average values in precipitation; starting from a positive anomaly in annual precipitation of  $+7.7\%$  at  $0\% \text{Geo}$  and decreasing with progressive application of SRM to  $-11.8\%$  at  $100\% \text{Geo}$ . Annual precipitation reaches pre-industrial values between  $40\%$  and  $50\%$  of full SRM deployment (Figure 2a), although the seasonality of rainfall has changed with relatively more rainfall in Autumn and Winter than Spring and Summer at  $40\text{--}50\%$ . The East

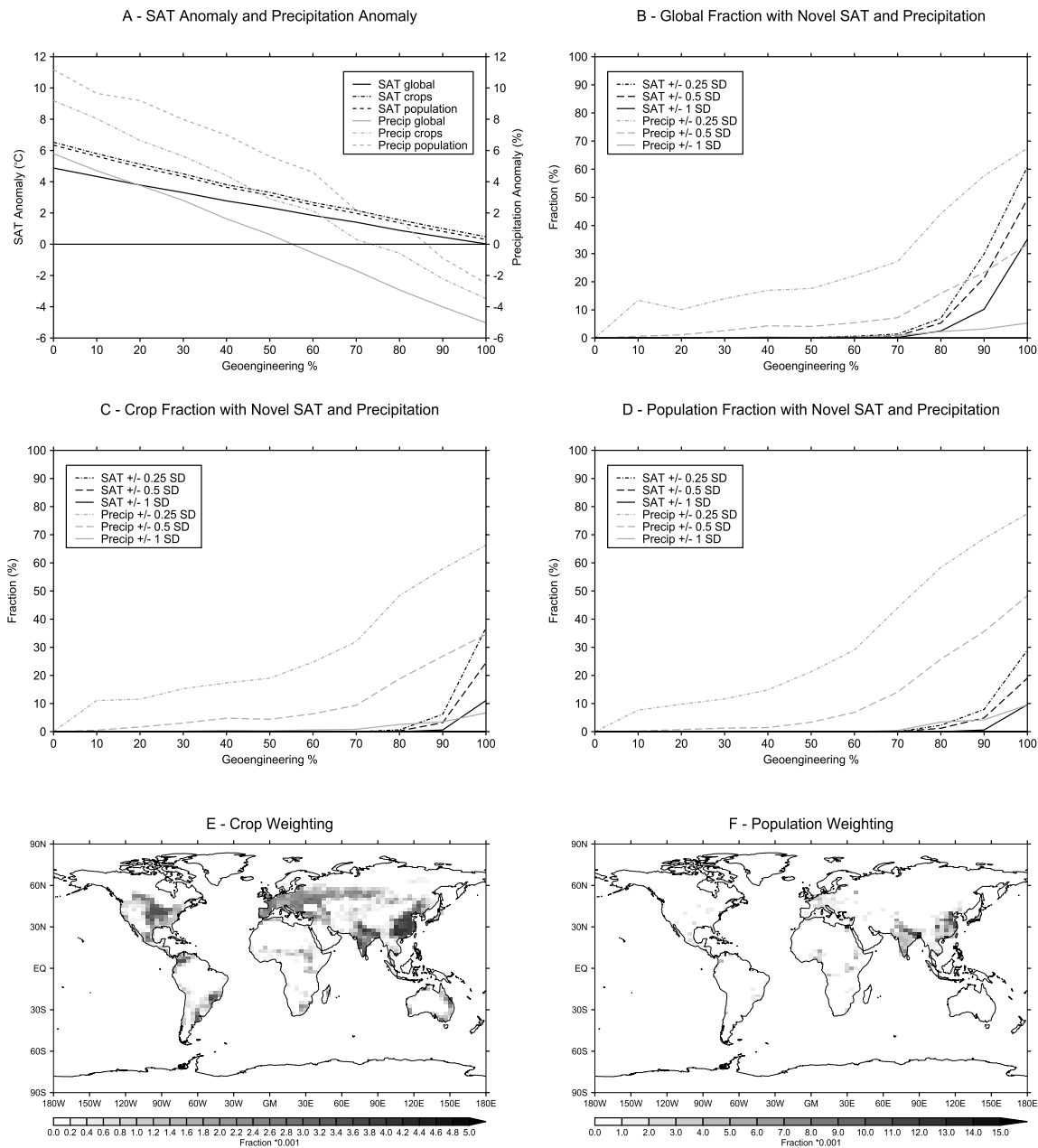


**Figure 3.** (a) The average surface air temperature (SAT) and precipitation (Precip) anomaly with the pre-industrial control as a function of the level of geoengineering, for the global average, weighted by crop area or by population. (b–d) The fraction of the global area (Figure 3b), crop area (Figure 3c), or population (Figure 3d) which experience novel SAT and precipitation conditions as a function of the level of SRM geoengineering (see text for description). (e and f) The crop area and population weighting applied to calculate the above.

Chinese (Figure 2b) region experiences a +28.6% increase in annual precipitation under unmitigated greenhouse warming (0%Geo) compared to pre-industrial which decreases under SRM geoengineering, returning to close to the pre-industrial annual average (−0.9% reduction) and seasonality (aside from a slightly drier spring) at 100%Geo. The Brazilian and Australian regions (Figures 2c and 2d) display large reductions in annual precipitation at 0%Geo which is ameliorated, to a greater or lesser extent, by increasing levels of SRM. The Australian region shows a complete recovery from a 28.0% reduction in annual precipitation at 0%Geo and returns to the pre-industrial average at 100%Geo. The

Brazilian region shows a lesser recovery from −34.8% to −9.5%. In the Western European region (Figure 2e) there is a shift to a much drier summer and a wetter winter at 0%Geo and under increased levels of SRM this shifts and the pre-industrial seasonality is restored however, overall the Western European region shows relatively little response in annual average precipitation to SRM deployment. It should be noted that despite using 100 year averages to calculate the climate state there will still be a degree of natural variability in these results.

[10] Even at the aggregation level of the regions discussed above, important smaller scale impacts may still be

obscured. Moreover, geoengineering impacts will differ substantially in socio-economic terms according to the relationship between climatic change and for example, distributions of population and cropland. We have thus explored an alternative means of assessing the regionality of the climate response to geoengineering, retaining the impacts calculated at the native resolution of the climate model ( $3.75^\circ$  longitude by  $2.5^\circ$  latitude [Cox *et al.*, 2000]), but calculating a single index by weighting the impacts according to specific 'recipients'. To illustrate, we present analysis weighted on a cropland fractional area and population density (per capita) basis, i.e. the impact on a small, highly cultivated region would be equal to the same impact on a large expanse of lightly cultivated land if they contained the same total area of crops, whilst two regions with the same intensity of cultivation would be weighted in direct proportion to their area. Figures 3e and 3f show the fraction of global crop area and population, at the resolution of the GCM model, used to generate this weighting.

[11] Figure 3a summarizes the changes in global average temperature and precipitation as well as average changes over crop area and populated areas. The crop area is calculated from the distribution of C3 and C4 grasses in managed regions derived from the Wilson and Henderson-Sellers vegetation cover dataset [Wilson and Henderson-Sellers, 1985] and the population distribution is derived from the LandScan 2007 population dataset [LandScan<sup>TM</sup>, 2007]. At 0%Geo, compared to pre-industrial, globally there is a  $4.87^\circ\text{C}$  warming and a 5.8% increase in precipitation whereas at 100%Geo there is a return to the pre-industrial temperature and a 5% reduction in the average precipitation [Lunt *et al.*, 2008]. To return average annual precipitation to the pre-industrial value globally would require ~55% of full geoengineering deployment. However, this figure is ~75% for crop regions and ~85% for populated areas.

[12] Even weighting by crop area/population density will mask disparities in regional precipitation and hence 'winners' and 'losers' of SRM geoengineering. We therefore introduce the concept of a 'novel' climate, which we define as the existence of a climatic state, measured by either surface temperature or rainfall (annual or seasonal), that lies outside the continuum of climatic states bounded by the pre-industrial and an unmitigated ( $\times 4$  CO<sub>2</sub>) greenhouse. For example, for a full SRM deployment, we would class the cooler-than-pre-Industrial tropics [Brovkin *et al.*, 2009; Govindasamy *et al.*, 2003] as constituting a 'novel' climate. However, to give a reasonable margin of error and to account for inter-annual variability we require the mean geoengineered climate state to exceed a threshold, based on the standard deviation of pre-industrial or unmitigated ( $\times 4$  CO<sub>2</sub>) climate variability, before it is classed as 'novel'. Figures 3b, 3c, and 3d show the fraction of the global area (Figure 3b), crop area (Figure 3c) and population (Figure 3d) which are affected by a novel climate at each level of SRM for 3 different thresholds, i.e. a climate state that is beyond 0.25, 0.5 and 1.0 standard deviations of the upper/lower bound. For global aggregation (Figure 3b), we find, using the lowest threshold ( $\pm 0.25$  SD), that for all levels of geoengineering some regions are affected by a novel precipitation, with 67% of the world affected at 100%Geo. With a more stringent threshold for a novel precipitation, the fractions affected are much lower, 33% for the mod-

erate threshold ( $\pm 0.5$  SD) 5% for the highest threshold ( $\pm 1.0$  SD). For crop area aggregation (Figure 3c) there is little change from the global picture but for population aggregation (Figure 3d) there is an increase in the affected fraction at higher levels of geoengineering for all threshold levels. Novel (cool) temperature conditions occur in the global analysis at around 70–80%Geo with 61% of the earth affected at the lowest threshold, dropping somewhat to 35% affected at the highest threshold. For both crop area (Figure 3c) and population (Figure 3d) aggregation a smaller fraction is affected by the cooler temperatures, this is due to the cooling mainly occurring in tropical and ocean areas.

#### 4. Discussion and Conclusions

[13] GCMs have model-specific biases, particularly with respect to precipitation changes at the regional and seasonal scales, and this will be reflected in assessments of geoengineering impacts. Even at the global scale, it is noticeable that models differ in the percentage (or absolute  $\text{W m}^{-2}$ ) reduction in the solar constant needed to cancel out a given elevation of CO<sub>2</sub> (e.g.,  $\times 4$ ). For instance, Govindasamy *et al.* [2003] find that to offset the warming of a quadrupling of CO<sub>2</sub> compared to pre-industrial, a 3.6% reduction in insolation is required, compared to our estimate of 4.2%. This difference likely reflects inter-model differences in climate sensitivity, because many of the same climate feedbacks will operate in response to both changes in incoming shortwave radiations and CO<sub>2</sub>. The warming of  $4.02^\circ\text{C}$  reported by Govindasamy *et al.* [2003] at  $4 \times \text{CO}_2$  compared to  $4.87^\circ\text{C}$  in this study is in approximately the same proportion as the solar constant change, supporting our interpretation. Precipitation patterns are not as well modeled in GCMs as temperature patterns and so our results should be viewed with this in mind [IPCC, 2007]. The GCM ensemble used in the IPCC's 4th report reproduced the observed zonal mean distribution of precipitation well and captured the major regional precipitation patterns (e.g. maxima over rainforests), but there were deficiencies in the ensemble's estimates for tropical precipitation, particularly in the tropical Atlantic and around the Bay of Bengal and the Maritime continent [IPCC, 2007]. When predicting precipitation changes as a result of global warming by the end of the 21st century, the magnitude of the change varies between GCMs with agreement on the sign of the change in most regions, with most of the disagreement in the mid-latitudes [IPCC, 2007].

[14] Furthermore, although the coupled GCM we used, HadCM3L, has been used in studies of future and past climates [e.g., Cox *et al.*, 2000; Lunt *et al.*, 2007], it has a relatively low resolution compared to many models used in the 4th Assessment Report [IPCC, 2007]. We have also chosen to keep vegetation fixed at pre-industrial values in the simulations in this study, therefore neglecting vegetation-climate feedbacks.

[15] If SRM geoengineering were to be implemented, it is apparent that it need not be deployed fully (i.e., to return global average temperatures to the pre-industrial value) and alternative mitigation objectives such as ensuring a neutral surface mass balance of the Greenland ice sheet [Oppenheimer and Alley, 2005] might be considered. For instance, we have previously found [Irvine *et al.*, 2009] that the level of SRM geoengineering required to prevent any

melting of the Greenland ice sheet in the Glimmer ice-sheet model [Rutt *et al.*, 2009] was 60%Geo or above, with a partial ice sheet maintained with interventions of 30%Geo to 50%Geo. Note however that the model used here, does not account for fast-flow ice dynamics [Rutt *et al.*, 2009], which played a dominant role in the variation in Greenland ice-sheet mass balance over the 20th century [Rignot *et al.*, 2008]. Restricting to only partial deployment may also avoid the occurrence of a significant area being affected by novel climates and hence adverse impacts.

[16] Although the results presented here are illustrative rather than predictive *per se*, and need to be replicated with higher resolution GCMs and ideally in multi-model ensembles, they indicate that it might be possible to identify a level of SRM geoengineering sufficient to maintain the Greenland ice sheet and cool the climate significantly via SRM, but without a large reduction in global precipitation and exposing only a small fraction of the Earth to novel climates. Clearly, a comprehensive cost-benefit analysis covering the impacts on agriculture, biodiversity, human health and other factors would also be required to assess adequately any proposed SRM geoengineering intervention.

[17] **Acknowledgments.** P.I. is funded on a NERC Ph.D. studentship. A.R. acknowledges support from The Royal Society in the form of a university research fellowship. D.L. acknowledges funding from the British Antarctic Survey and from the RCUK in the form of a research fellowship.

## References

- Angel, R. (2006), Feasibility of cooling the Earth with a cloud of small spacecraft near the inner Lagrange point (L1), *Proc. Natl. Acad. Sci. U. S. A.*, 103(46), 17,184–17,189, doi:10.1073/pnas.0608163103.
- Anthoff, D., C. Hepburn, and R. S. J. Tol (2009), Equity weighting and the marginal damage costs of climate change, *Ecol. Econ.*, 68(3), 836–849, doi:10.1016/j.ecolecon.2008.06.017.
- Bala, G., P. B. Duffy, and K. E. Taylor (2008), Impact of geoengineering schemes on the global hydrological cycle, *Proc. Natl. Acad. Sci. U. S. A.*, 105(22), 7664–7669, doi:10.1073/pnas.0711648105.
- Brovkin, V., V. Petoukhov, M. Claussen, E. Bauer, D. Archer, and C. Jaeger (2009), Geoengineering climate by stratospheric sulfur injections: Earth system vulnerability to technological failure, *Clim. Change*, 92(3–4), 243–259, doi:10.1007/s10584-008-9490-1.
- Cox, P. M., R. A. Betts, C. D. Jones, S. A. Spall, and I. J. Totterdell (2000), Acceleration of global warming due to carbon-cycle feedbacks in a coupled climate model, *Nature*, 408(6809), 184–187, doi:10.1038/35041539.
- Crutzen, P. J. (2006), Albedo enhancement by stratospheric sulfur injections: A contribution to resolve a policy dilemma?, *Clim. Change*, 77(3–4), 211–220, doi:10.1007/s10584-006-9101-y.
- Govindasamy, B., K. Caldeira, and P. B. Duffy (2003), Geoengineering Earth's radiation balance to mitigate climate change from a quadrupling of CO<sub>2</sub>, *Global Planet. Change*, 37(1–2), 157–168, doi:10.1016/S0921-8181(02)00195-9.
- Hansen, J., M. Sato, R. Ruedy, K. Lo, D. W. Lea, and M. Medina-Elizade (2006), Global temperature change, *Proc. Natl. Acad. Sci. U. S. A.*, 103(39), 14,288–14,293, doi:10.1073/pnas.0606291103.
- Intergovernmental Panel on Climate Change (IPCC) (2007), *Climate Change 2007: The Physical Science Basis: Contribution of Working Group I to the Fourth Assessment Report of the Intergovernmental Panel on Climate Change*, edited by S. Solomon *et al.*, 996 pp., Cambridge Univ. Press, New York.
- Irvine, P. J., D. J. Lunt, E. J. Stone, and A. Ridgwell (2009), The fate of the Greenland Ice Sheet in a geoengineered, high CO<sub>2</sub> world, *Environ. Res. Lett.*, 4(4), 045109, doi:10.1088/1748-9326/4/4/045109.
- LandScan™ (2007), Global population database, <http://www.ornl.gov/sci/landscan/>, Oak Ridge Natl. Lab., Oak Ridge, Tenn.
- Lenton, T. M., and N. E. Vaughan (2009), The radiative forcing potential of different climate geoengineering options, *Atmos. Chem. Phys.*, 9(15), 5539–5561, doi:10.5194/acp-9-5539-2009.
- Lenton, T. M., H. Held, E. Kriegler, J. W. Hall, W. Lucht, S. Rahmstorf, and H. J. Schellnhuber (2008), Tipping elements in the Earth's climate system, *Proc. Natl. Acad. Sci. U. S. A.*, 105(6), 1786–1793, doi:10.1073/pnas.0705414105.
- Lunt, D. J., I. Ross, P. J. Hopley, and P. J. Valdes (2007), Modelling late Oligocene C-4 grasses and climate, *Palaeogeogr. Palaeoclimatol. Palaeoecol.*, 251(2), 239–253, doi:10.1016/j.palaeo.2007.04.004.
- Lunt, D. J., A. Ridgwell, P. J. Valdes, and A. Seale (2008), "Sunshade World": A fully coupled GCM evaluation of the climatic impacts of geoengineering, *Geophys. Res. Lett.*, 35, L12710, doi:10.1029/2008GL033674.
- Matthews, H. D., L. Cao, and K. Caldeira (2009), Sensitivity of ocean acidification to geoengineered climate stabilization, *Geophys. Res. Lett.*, 36, L17066, doi:10.1029/2009GL037488.
- Oppenheimer, M., and R. B. Alley (2005), Ice sheets, global warming, and Article 2 of the UNFCCC, *Clim. Change*, 68(3), 257–267, doi:10.1007/s10584-005-5372-y.
- Rignot, E., J. E. Box, E. Burgess, and E. Hanna (2008), Mass balance of the Greenland ice sheet from 1958 to 2007, *Geophys. Res. Lett.*, 35, L20502, doi:10.1029/2008GL035417.
- Robock, A., A. Marquardt, B. Kravitz, and G. Stenchikov (2009), Benefits, risks, and costs of stratospheric geoengineering, *Geophys. Res. Lett.*, 36, L19703, doi:10.1029/2009GL039209.
- Rutt, I. C., M. Hagdorn, N. R. J. Hulton, and A. J. Payne (2009), The Glimmer community ice sheet model, *J. Geophys. Res.*, 114, F02004, doi:10.1029/2008JF001015.
- Wilson, M. F., and A. Henderson-Sellers (1985), A global archive of land cover and soils data for use in general-circulation climate models, *J. Climatol.*, 5(2), 119–143, doi:10.1002/joc.3370050202.

P. J. Irvine, D. J. Lunt, and A. Ridgwell, Bristol Research Initiative for the Dynamic Global Environment, School of Geographical Sciences, University of Bristol, Bristol BS8 1SS, UK.